Application of Deep Learning to Detection and Survival Prediction of COVID-19 Patients Based on Lung X-Ray Images

Barry B. Barrios
barriosb@stanford.edu

Michal Maciejewski
mmacieje@stanford.edu

Bhavik Shah
bas336@stanford.edu

***Category*—** Healthcare

Abstract

In this contribution we discuss the application of deep learning methods to study 2D X-Ray images of COVID-19 patients. In particular, we employ a convolutional neural network (CNN) to classify X-ray images into three classes: normal, viral pneumonia and COVID-19. For X-Rays classified as COVID-19 we perform manual and automatic temporal progression analysis. For the manual analysis we display a series of X-Ray scans containing the most similar feature embedding under the cosine similarity. Furthermore, by studying a series of images of a given patient with a sequence model (long-short term memory RNN), we investigate the survival rate. Various experiments are reported along with comparison of model performance.

1 Problem Description

The COVID-19 pandemic has had an unprecedented impact on the humanity. We intend to contribute to the global data-driven modelling effort and support classification of X-Ray images of COVID-19 patients as well as study their survival. We envisage to approach our problem in two stages with growing model complexity. The input, in the first stage, are X-Ray images of COVID-19 patients as well as patients with other lung diseases along with healthy individuals. For the purpose of this study we consider two-dimensional images (2D). The output of the first stage is a binary model implemented with a CNN, which outputs a probability on whether a patient has COVID-19. The second stage requires the input of time-series data, namely the progression of COVID-19 in the X-Rays. Then, given the patient has the disease, we will output the survival rate.

1.1 Related work

Currently, existing data sets are analyzed with deep learning methods (especially image detection and classification). Given the global climate, detection is a huge part of novel work being carried out. Usually this is done with CNNs on X-Ray images (see [1], [2], [3], [4], [5]), which is generally the path that we will follow. Another approach involves deep learning decision-tree classifiers (cf. [6]). In the field of survival rate prediction, we identified several relevant pieces of research work on COVID-19, e.g., [7], [8]. Wang et al. used a CNN to discover tumor shape and predict survival in patients with lung cancer [9]. Deep NNs were also used for survival prediction in brain tumors [10]. DeepSurv [11] uses a Cox proportional hazard deep neural network to recommend a personalized treatment. The novelty of our work is use of CNN and LSTM to survival prediction.

2 Dataset

Data gathering was a challenge as a lot of data is being collected right now, albeit not necessarily cleaned. We also had an issue in terms of time evolution of the X-Ray scans, where there is not a lot of open data sets tracking the progression of the disease. Particularly, in comparison with healthy patients which is desired for us to train the sequential part of our model. Some articles, such as [1], even generate their own images given the lack of robust data sets. Data is often conflated with pneumonia data sets, so our goal is to detect COVID-19 in cases where the pneumonia is not as pronounced.

Initially, we selected a data set available at Kaggle [12] comprising of three data sets: (i) normal; (ii) viral pneumonia; (iii) COVID-19 [13]; see Fig. 1. Table 1 shows a count of examples per class.

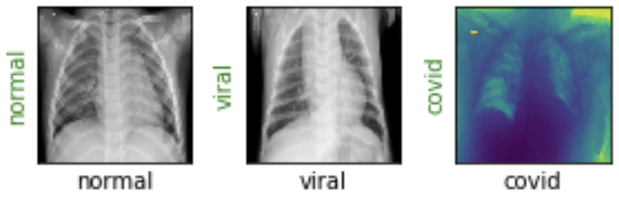

Figure 1: Examples of X-Ray scans from the data set for normal, viral pneumonia and COVID-19 classes (from left to right).

Normal	Pneumonia	COVID-19
1341	1345	219

Table 1: Count of training examples per class in the imbalanced data set.

In order to improve the learning process we collected more X-Ray scans of COVID-19 patients. Initially, we collected additional 112 X-Ray scans from SIRM [14] and Radiopaedia [15] published after the first data set was made available. Furthermore, we found a new data set containing X-Ray and CT scans of 1,311 patients from Valencia, Spain [16]. The data set required cleaning of image names, filtering out lateral scans (by manual labeling) and CTs (automatically by file extension) as well as converting the palletised PNG format into a three-channel RGB one. Eventually, we enhanced our data set by 3037 COVID-19 scans. Note that typically a patient has several X-Ray scans corresponding to several sessions allowing to follow the disease progression. The count of classes in the balanced data set is given in Table 2.

Normal	Pneumonia	COVID-19
1341	1345	1345

Table 2: Count of training examples per class in the balanced data set.

3 Modelling Approach

Our modelling approach is divided into two main steps: (i) multi-class classification; and (ii) time progression analysis. For the multi-class classification we begin with transfer learning for two well-established CNN architectures, namely ResNet18 and DenseNet50. Moreover, we employ a custom network dedicated to the classification of X-Ray scans [17]. Once a scan is labeled as COVID-19 we proceed into time progression analysis. This step is divided into a manual and automatic mode. For the manual mode we use the feature embedding from the classifier (input of the last fully-connected layer). Given an X-Ray we provide the most similar scan along with its temporal progression and description. For the automatic mode, we employ a CNN and LSTM networks to predict survival of a patient. The summary of our modelling approach is given in Fig. 2. We split the data set into 80% training, 10 % development, and 10 % test.

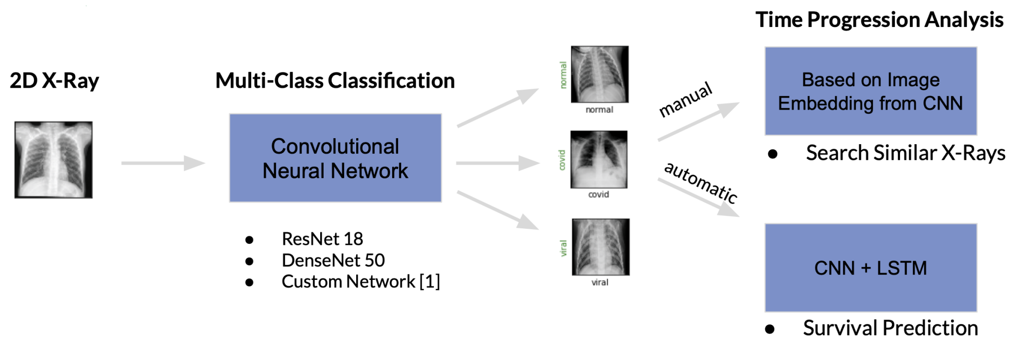

Figure 2: Modelling approach for detection and survival prediction of COVID-19 Patients based on lung X-Ray images.

3.1 Multi-Class Classification

We chose the pytorch library to train a multi-class classifier. The classifier labels normal X-Ray scans and two classes of scans indicating a viral disease (either pneumonia or COVID-19). We decided to follow a similar path as reported in literature by performing transfer learning on a pre-trained CNN (ResNet and DenseNet). The new approach was to re-implement a custom model used in another study of X-Ray scans [17]. For the classical CNN models, we performed the hyperparameter tuning and studied the impact of these changes on the model performance.

3.1.1 ResNet Architecture

We carried out first experiments with the ResNet-18 architecture used for image classification tasks. The model had pre-trained parameters on the ImageNet dataset. We modified the output, fully connected layer in order to classify images into three classes (normal, COVID-19, pneumonia). We used an ADAM optimization technique with a learning rate of $3*10^{-5}$ and a binary cross-entropy loss. Experiments for the imbalanced data set are reported in Appendix B.

With the balanced data set, we began with a tuning of the batch size. After observing the loss evolution for several batch sizes (6, 12, 18, 24), we concluded that the fastest training and lowest loss after 20 epochs was achieved for a batch of 24 images; see Fig 3.

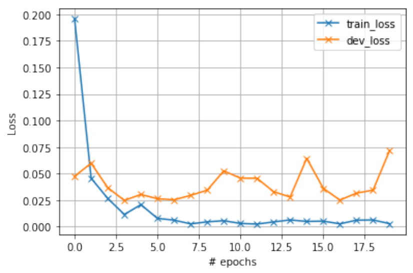

Figure 3: Learning curve for Resnet18 model with the balanced data set and the batch size of 24 images.

	N	V	C
N	121	14	0
V	2	133	0
C	0	0	135

Table 3: Confusion matrix for Resnet18 model with the balanced data set and the batch size of 24 images.

In this case an early stopping strategy could reduce the over-fitting of the model. From Table 3 we note that the model did not commit any error on the test set for COVID-19 examples; in the paper we follow a convention that columns denote predicted labels and the rows contain the true labels. Therefore, we decided to take this classifier as a reference one for the manual time progression analysis.

3.1.2 DenseNet Architecture

We performed several experiments with the DenseNet-121 architecture used for image classification tasks. In the first experiment, we used the pre-trained parameters and we froze all the weights in all the layers except for the last layer composed of a custom trainable classifier consisting of a ReLu, adaptive avg pool2d and a flatten followed by a softmax classifier layer. After training for 20 epochs, the model was able to predict all three classes: Normal, Viral, and Covid. Please refer to Appendix C for the detailed results.

3.1.3 Custom Architecture

We now leverage the structure utilized in [18] in order to build a CNN for classifying the lung x-rays. This structure feeds the data through a number of simple convolutional blocks. The two main parameters we ended up controlling in this facet of the problem were the number of blocks to use as well as the learning rate. We first find that adding one more block on top of original architecture (which used 5) allowed us to increase the training dev accuracy by about 10%. Past this, we start to see a split where we begin to overfit on the training data. Moreover, after finding a feasible lower and upper bound for the learning rate, we did an iterative search over possible values and found that a learning rate of $\alpha = 3 * 10^{-5}$ gives us pretty good convergence. We see that using these hyperparameters, we gain a training accuracy of 99.69% and a dev accuracy of 93.58%. Note that still, there is a degree of overfitting in our model, despite that we've tried to control this. Similarly to the issues experienced in Section 3.1.1, we see from inspecting the curve that early stopping might help us aleviate this problem.

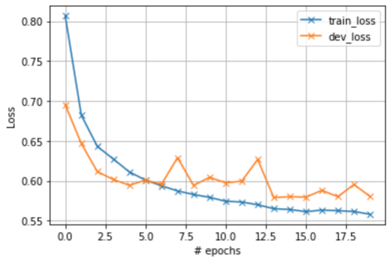

Figure 4: Learning curve for custom architecture with the balanced data set.

	N	V	C
N	119	16	0
V	6	128	1
C	0	3	132

Confusion Matrix for Custom Model

3.2 Time Progression Analysis

Once an X-Ray is classified as a COVID-19 class, we perform time progression analysis. The goal of the analysis is to predict the progression of the disease based on the actual scan. We approach this task with a manual and automatic methods.

3.2.1 X-Ray Search with Image Embedding

Based on the ResNet18 model with the best performance we perform a forward propagation for each of the COVID-19 scans and extract embedding as an input vector of the last fully connected layer. The input vector is composed of 512 elements. Given an input image we return a list of n most similar image sets with respect to the cosine similarity $S(u, v) = u^T v/||u|| * ||v||$, where u and v are X-ray embeddings. The image set consists of a series of images of a given patient taken over time. This allows to manually compare the images and infer about the progression of the disease. Furthermore, we display a radiologist annotation for each X-ray scanning session. Naturally, this method is only suited for experienced radiologists and medical doctors.

3.2.2 Survival Analysis with Sequence Model

We proposed a time-distributed CNN-LSTM architecture as shown in Figure 5, which incorporates the temporal relationship between different X-Ray images from the same patient, as a patient can take many scans sequentially over time during their hospital stay to monitor changes of the disease.

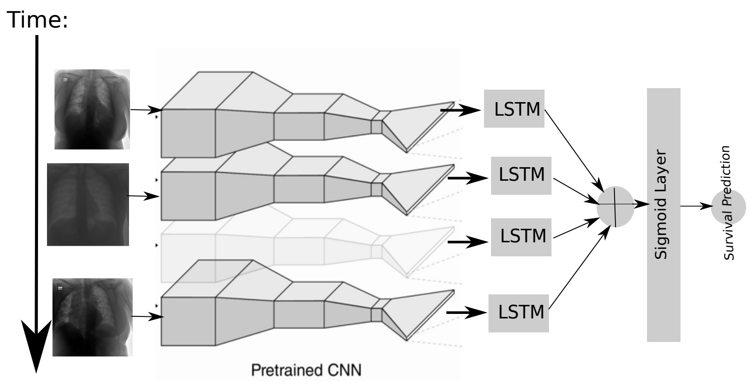

Figure 5: Proposed CNN-LSTM Architecture

This proposed architecture is able to evaluate the Covid-19 evolution by learning the temporal correlations of images provided as input. We demonstrate that this model can integrate imaging scans at multiple timepoints to predict chances of survival. One CNN is defined at each timepoint input, which learns the spatial features of the image. The output of the pre-trained CNN network is then fed into an LSTM which is used to learn the temporal relationship across the series of images. The final sigmoid layer allows for a binary classification output (dead/survived). In our implementation of the CNN part of our architecture, we used a pre-trained DenseNet121 model and applied a 2D adaptive average pooling followed by a FC-1024 layer. An LSTM is then applied by defining 64 hidden units followed by a sigmoid layer to perform binary classification. We used an ADAM optimization technique with a learning rate of 0.01 and a binary cross-entropy loss. The momentum value was set to 0.5. Figure 6 shows the confusion matrix of our survival prediction results.

(a) Confusion matrix of CNN-LSTM model with normalization

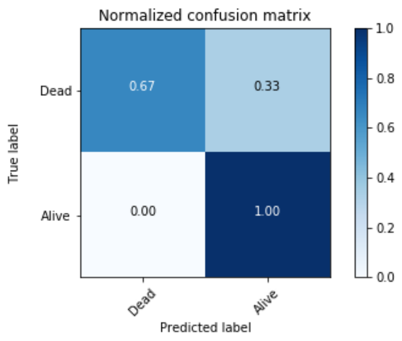

(b) Confusion matrix of CNN-LSTM model without normalization

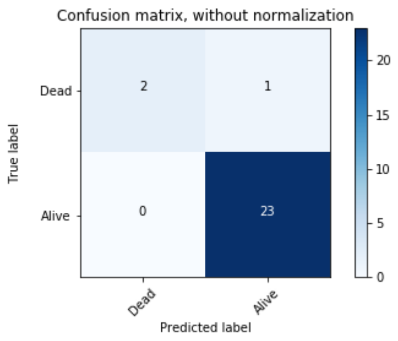

Figure 6: Confusion Matrix for Survival Model

Two time series of a Covid-19 patient with a survival probability of 0.9330 using the raw X-ray images are shown in Figure 7 (a-b). As one can notice, over time the state of the patient improved (lungs are not covered with inflammation) and lungs are more visible; this is confirmed by indication of our model. Figure 7 (c-e) shows three activation maps for different time periods for subject s03113 with a predicted survival probability of 0.8438 calculated by the sigmoid function. Note highlight of the model activation overlayed over the scan.

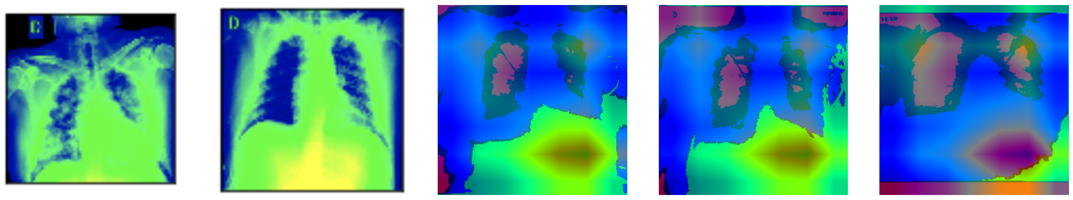

(a) first (b) second (c) day 1 (d) day 5 (e) day 8

Figure 7: (a-b) COVID-19 pneumonia - timeline for Subject sub-S03213 with survival probability of 0.9330; (c-e) COVID-19 pneumonia - timeline for Subject sub-S03113 with survival probability of 0.8438

4 Conclusion

Through this project, we have utilized a robust and principled workflow in order to create a system that is able to (1) discern cases of COVID-19, and (2) generate a survival prediction. For the multi-class classification we employed both transfer learning (ResNet, DenseNet) as well as a custom architecture suited to X-Ray classification. For each model we performed hyperparameter tuning in order to reduce overfit while maintaining high accuracy. In both the setting where we create a custom model and utilize a pre-trained model with slight modifications, we were able to achieve a high (>90%) accuracy rate on all classes in the test set. However, the one caveat is that we see a reasonable degree of variance, since again in both cases, we have a training accuracy of close to 100%. One of the modelling challenges was an imbalanced dataset (low number of COVID-19 cases). In that respect, incorporation of an additional dataset allowed to obtain meaningful results while various strategies for handling class imbalance were not as effective.

For X-Ray scans labeled as COVID-19 we performed time progression analysis. X-ray embedding allowed for search of similar COVID-19 cases in an annotated database. Survival prediction model combined CNN and LSTM and provided good accuracy in predicting the disease progression.

Future work will focus on applying different CNN models (DenseNet201, VGG16, VGG19, Inception-v3, etc.) on our proposed CNN-LSTM architecture. We can also incorporate demographic, clinical, and laboratory data to predict mortality and the need for ventilator support.

Acknowledgment

Firstly we would like to thank Shahab Mousavi for overlooking the project as well as other CS230 TAs for help at various stages. Initial work was carried out with free GPU instances delivered by Google Colab. The training of classification and survival prediction models on the balanced dataset was possible due to credits provided by Amazon AWS.

References

[1] Zebin T and Rezvy S. Covid-19 detection and disease progression visualization: Deep learning on chest. *Appl Intell*, 2020.

[2] Shervin Minaee, Rahele Kafieh, Milan Sonka, Shakib Yazdani, and Ghazaleh Jamalipour Soufi. Deep-covid: Predicting covid-19 from chest x-ray images using deep transfer learning. *Medical Image Analysis*, 65:101794, 2020.

[3] Cohen J, Dao L, and Roth K et al. Predicting covid-19 pneumonia severity on chest x-ray with deep learning. *Cureus*, 2020.

[4] Harsh Panwar, P.K. Gupta, Mohammad Khubeb Siddiqui, Ruben Morales-Menendez, Prakhar Bhardwaj, and Vaishnavi Singh. A deep learning and grad-cam based color visualization approach for fast detection of covid-19 cases using chest x-ray and ct-scan images. *Chaos, Solitons & Fractals*, 140:110190, 2020.

[5] Butt C., Gill J., Chun D., and Babu B. A. Deep learning system to screen coronavirus disease 2019 pneumonia. *Applied Intelligence*, 2020.

[6] Seung Hoon Yoo, Hui Geng, Tin Lok Chiu, Siu Ki Yu, Dae Chul Cho, Jin Heo, Min Sung Choi, Il Hyun Choi, Cong Cung Van, Nguen Viet Nhung, Byung Jun Min, and Ho Lee. Deep learning-based decision-tree classifier for covid-19 diagnosis from chest x-ray imaging. *Frontiers in Medicine*, 7:427, 2020.

[7] J. P. et al Cohen. "predicting covid-19 pneumonia severity on chest x-ray with deep learning". *Cureus*, 2020.

[8] Alfonso Emilio Gerevini, Roberto Maroldi, Matteo Olivato, Luca Putelli, and Ivan Serina. Prognosis prediction in covid-19 patients from lab tests and x-ray data through randomized decision trees, 2020.

[9] Wang S., Chen A., and Yang L. et al. Comprehensive analysis of lung cancer pathology images to discover tumor shape and boundary features that predict survival outcome. *Scientific Reports*, 2018.

[10] Po-Yu Kao, Thuyen Ngo, Angela Zhang, Jefferson W. Chen, and B. S. Manjunath. Brain tumor segmentation and tractographic feature extraction from structural mr images for overall survival prediction. In Alessandro Crimi, Spyridon Bakas, Hugo Kuijf, Farahani Keyvan, Mauricio Reyes, and Theo van Walsum, editors, *Brainlesion: Glioma, Multiple Sclerosis, Stroke and Traumatic Brain Injuries*, pages 128–141, Cham, 2019. Springer International Publishing.

[11] Katzman Jared L. et al. Deepsurv: personalized treatment recommender system using a cox proportional hazards deep neural network. *BMC medical research methodolog*, 2018.

[12] COVID-19 Radiography Database, `https://www.kaggle.com/tawsifurrahman/covid19-radiography-database`.

[13] Cohen J.P., Morrison P., and Dao L. Covid-19 image data collection, 2020.

[14] SIRM COVID-19 Database, `https://www.sirm.org/category/senza-categoria/covid-19/`.

[15] Radiopaedia covid-19, `https://radiopaedia.org/articles/covid-19-4`.

[16] Maria de la Iglesia Vayá, Jose Manuel Saborit, Joaquim Angel Montell, Antonio Pertusa, Aurelia Bustos, Miguel Cazorla, Joaquin Galant, Xavier Barber, Domingo Orozco-Beltrán, Francisco García-García, Marisa Caparrós, Germán González, and Jose María Salinas. Bimcv covid-19+: a large annotated dataset of rx and ct images from covid-19 patients, 2020.

[17] F. Pasa, V. Golkov, and F. et al Pfeiffer. Efficient deep network architectures for fast chest x-ray tuberculosis screening and visualization. *Sci Rep*, 2019.

[18] F. Pasa et al. Efficient deep network architectures for fast chest x-ray tuberculosis screening and visualization. *Scientific Reports*, 2019.

[19] Data Preparation Notebook, https://github.com/michalmac89/cs230finalproject/blob/dropout/Pytorch_COVID_19_Data_Preparation.ipynb.

[20] Covid-19 detection x-ray, https://www.coursera.org/projects/covid-19-detection-x-ray.

[21] Model Training Notebook, https://github.com/michalmac89/cs230finalproject/blob/dropout/Pytorch_COVID_19_ResNet18_Dropout.ipynb.

[22] Post-Processing Notebook, https://github.com/michalmac89/cs230finalproject/blob/dropout/Post_Processing_ResNet_18_Dropout.ipynb.

[23] Transfer Learning DenseNet121 Notebook, https://github.com/michalmac89/cs230finalproject/blob/main/DenseNet_Transfer_Learning.ipynb.

[24] Imbalanced Dataset Sampler Resnet18 Notebook, https://github.com/michalmac89/cs230finalproject/blob/main/Pytorch_COVID_19_ResNet18_Model_With_under_and_over_sampling.ipynb.

A Workflow

Our primary goal was to establish a workflow to query the data set, set-up and train model as well as compare and evaluate results. Since the data set is relatively small we decided to carry out all the steps in a Jupyter Notebook in Google Colab. This choice also enabled collaborative work.

We queried the data set from Kaggle to Google Colab space with the Kaggle Python API. After unpacking we moved the files to Google drive in order to preserve them between session. In addition, we split the data set into training, development, and test sets. To this end we created a notebook reported in [19].

Model training includes creating a data loader along with appropriate transformations and defining a training loop. We used cross-entropy loss and Adam optimizer for batch gradient descent.

Algorithm 1: Training loop

```
Result: Write here the result
initialization;
for each epoch do
    for each batch in the training set do
        calculate forward propagation;
        calculate cross-entropy loss;
        calculate backward propagation;
        update parameters;
    end
    compute and store a training loss for current epoch compute and store an accuracy for the training set
    for each batch in the dev set do
        calculate forward propagation;
        calculate cross-entropy loss;
    end
    compute and store a dev loss for current epoch compute and store an accuracy for the dev set
end
```

Once the training is completed, we run forward propagation on the tests set to evaluate final performance of the model. Each model has been evaluated on the following metrics: accuracy and confusion matrix evaluated for training and dev sets. The workflow is an extension of a case study presented in course [20].

B ResNet Experiments

The model was trained for 20 epochs with a batch of 6 images. For the reference model and imbalanced data set, we obtained 100 % and 96.6 % accuracy for the training and test sets, respectively. The difference in the accuracy indicates overfitting of the model. In fact, the model perfectly classified all training examples. Therefore, we added dropout in the final fully-connected layer and studied the model accuracy. Two cases were considered (80 % and 50 % probability of keeping weights in the model). 80 % dropout reduced the accuracy for both training (97.1 %) and development sets (97.8 %), thus, reducing model over fitting. Further increase of dropout probability to 50 % significantly deteriorated model performance: 83.1 % for training and 93.3 % for development sets. We note that due to a relatively large complexity of the model and a rather small data set (subject to class imbalance), the model tends to overfit the training examples. This translates into a difficulty in fine tuning the model. The notebook used for ResNet-18 studies is available at [21] and the post-processing notebook is stored in [22].

C DenseNet Experiments

Table from the first, second and third experiments (confusion matrix and the precision/recall/f1-score metrics)

	N	**V**	**C**
N	124	10	1
V	15	120	0
C	0	0	135

(a) First experiment

	N	**V**	**C**
N	124	10	1
V	15	120	0
C	0	0	135

(b) Second experiment

	N	**V**	**C**
N	131	4	0
V	2	133	0
C	0	2	133

(c) Third experiment

Table 4: Confusion Matrix for the three experiments; N stands for Normal class, C stands for COVID-19 class, and V stands for Viral Pneumonia Class.

All models were trained with a mini-batch size of 6 and for 20 epochs trying out different layers to freeze. In the first experiment we froze all the layers except the last layer. In the second experiment we froze just the first layer. We saw no difference between the first two experiments. In the last experiment we didn't freeze any of the layers. They more or less perform about the same. The notebook that implements the transfer learning of a pre-trained DenseNet is available at [23].

	precision	recall	f1-score	support
Normal	0.892086	0.918519	0.905109	135.000000
Viral	0.923077	0.888889	0.905660	135.000000
Covid	0.992647	1.000000	0.996310	135.000000
accuracy	0.935802	0.935802	0.935802	0.935802
macro avg	0.935937	0.935802	0.935693	405.000000
weighted avg	0.935937	0.935802	0.935693	405.000000

Table 5: Metrics for the first experiment

	precision	recall	f1-score	support
Normal	0.892086	0.918519	0.905109	135.000000
Viral	0.923077	0.888889	0.905660	135.000000
Covid	0.992647	1.000000	0.996310	135.000000
accuracy	0.935802	0.935802	0.935802	0.935802
macro avg	0.935937	0.935802	0.935693	405.000000
weighted avg	0.935937	0.935802	0.935693	405.000000

Table 6: Metrics for the second experiment

D Strategies for Handling Imbalanced Classes

The COVID-19 examples are under-represented in the dataset. Therefore, in the first attempt we decided to reduce to 300 the number of examples for normal and viral pneumonia classes. Afterwards, we utilized a combination of minority class over-sampling and majority class under-sampling to compensate for the imbalanced training dataset. It consisted of removing samples from the majority class (under-sampling) and/or adding more examples from the minority class (over-sampling).

With the imbalanced dataset sampler and after training for 90 epochs:

	precision	recall	f1-score	support
Normal	0.984962	0.970370	0.977612	135.000000
Viral	0.956835	0.985185	0.970803	135.000000
Covid	1.000000	0.985185	0.992537	135.000000
accuracy	0.980247	0.980247	0.980247	0.980247
macro avg	0.980599	0.980247	0.980317	405.000000
weighted avg	0.980599	0.980247	0.980317	405.000000

Table 7: Metrics for the third experiment

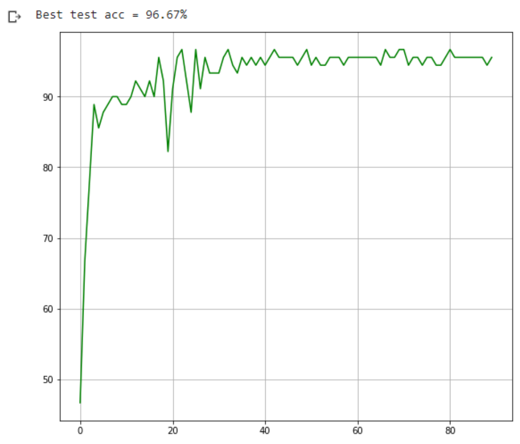

```
Best test acc = 96.67%
```

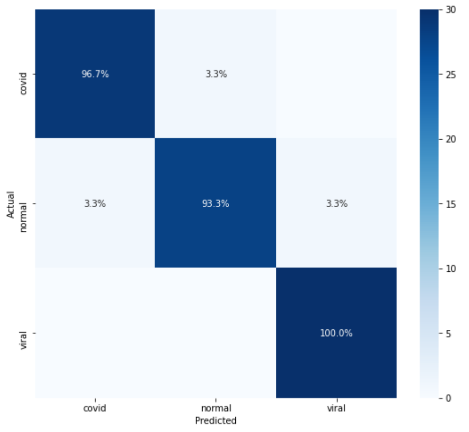

Without the imbalanced data set sampler and after training for 90 epochs:

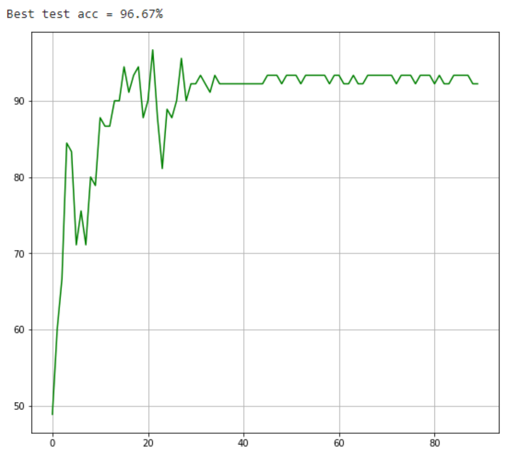

```
Best test acc = 96.67%
```

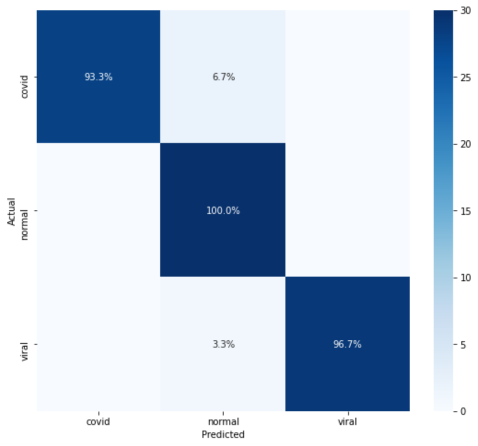

Note that there are significant improvements for the Covid class when applying both under-sampling and over-sampling strategies to deal with class imbalanced while the accuracy of the other classes were not impacted that much, i.e., the accuracy of the Covid class increased from 93.3% to 96.7% using the imbalanced dataset sampler. Take a look at the following notebook [24] that implements this random sampler for an imbalanced dataset.

E Survival Analysis

Figure 8 displays the accuracy and loss curves of our proposed CNN-LSTM model over 125 epochs.

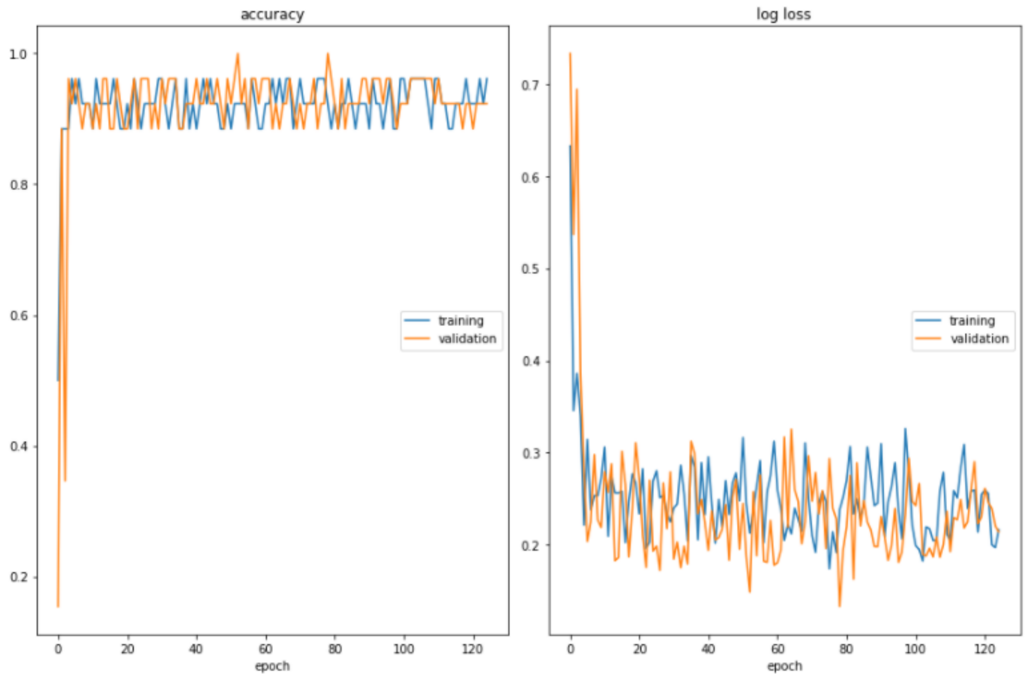

Figure 8: Accuracy/Loss of the CNN-LSTM model to predict survival with a Densenet121 pre-trained CNN